

Primer

Imaging Neurotransmitter and Neuromodulator Dynamics *In Vivo* with Genetically Encoded Indicators

Bernardo L. Sabatini^{1,*} and Lin Tian^{2,*}¹Howard Hughes Medical Institute, Department of Neurobiology, Harvard Medical School, Boston, MA, USA²Departments of Biochemistry and Molecular Medicine, School of Medicine, University of California, Davis, CA, USA*Correspondence: lintian@ucdavis.edu (L.T.), bernardo_sabatini@hms.harvard.edu (B.L.S.)<https://doi.org/10.1016/j.neuron.2020.09.036>

SUMMARY

The actions of neuromodulation are thought to mediate the ability of the mammalian brain to dynamically adjust its functional state in response to changes in the environment. Altered neurotransmitter (NT) and neuromodulator (NM) signaling is central to the pathogenesis or treatment of many human neurological and psychiatric disorders, including Parkinson's disease, schizophrenia, depression, and addiction. To reveal the precise mechanisms by which these neurochemicals regulate healthy and diseased neural circuitry, one needs to measure their spatiotemporal dynamics in the living brain with great precision. Here, we discuss recent development, optimization, and applications of optical approaches to measure the spatial and temporal profiles of NT and NM release in the brain using genetically encoded sensors for *in vivo* studies.

INTRODUCTION

Superimposed on the synaptic signaling that relays information from one neuron to another, there is a large set of neuromodulator (NM) signals mediated by the release of small molecules and neuropeptides. NMs exert profound influences on the activity of subsets of neurons, modulating global brain processes such as arousal, attention, or emotion, and thus animal behavior. Although the anatomical characterization and functional significance of NM-specific projections are understood to a moderate degree, the mechanisms by which these molecules regulate the dynamics of healthy and diseased neural circuitry are not fully understood. Gaining an understanding of these mechanisms requires sensitive, specific, and direct measurements of the type and magnitude of NM transients produced by their release with requisite spatiotemporal resolution in cell culture, tissue preparations, and intact circuits.

Analytical techniques have been broadly employed to directly measure extracellular concentrations of NMs, including neuropeptides, in the brain and have provided useful insights into the actions of NMs. For example, fast-scan cyclic voltammetry (FSCV) with carbon fiber microelectrodes can detect electrochemically active NMs, most notably dopamine (DA), in the nanomolar range and on the subsecond timescale (Wightman, 2006; Ganesana et al., 2017; Puthongkham and Venton, 2020; Venton and Cao, 2020). Furthermore, amperometric DA detection can provide absolute measurements, as charge is directly proportional to the number of oxidized DA molecules, and amperometry also enables quantal DA release detection at synapse in neuroendocrine cells such as adrenal chromaffin cells (Pothos et al., 1998).

However, FSCV-based detection of other biogenic amines, such as norepinephrine and serotonin, can be convoluted due

to the lack of specificity of electrochemical detection (i.e., multiple species are oxidized or reduced at overlapping potentials) (Heien et al., 2003). Alternatively, microdialysis measures neurochemicals *in vivo*, including those that are electrically inactive, by physically collecting chemicals from the living brain for post hoc analysis (Ungerstedt and Hallström, 1987; Kennedy, 2013; Ganesana et al., 2017; Frank et al., 2019). When coupled with sensitive analytical techniques, commonly mass spectrometry, liquid chromatography, or capillary electrophoresis, nanomolar to picomolar sensitivity can be achieved with great molecular specificity. However, the sensitivity of analytical methods sets limitations on the sample volume needed to detect target analytes and thus the necessary sampling time.

In addition, *in vivo* recordings using FSCV or microdialysis either suffer from low (compared to a submicron-scale release site) spatial resolution due to the large probe size (5–25 μm for carbon fiber electrodes and $\sim 100 \mu\text{m}$ for microdialysis probes) or likely cannot access the fast and rapid neurotransmitter (NT) and NM transients in synaptic clefts that occur at millisecond scales (Rodeberg et al., 2017; Ngernsutivorakul et al., 2018). Developments in FSCV and microdialysis have improved the temporal resolution, chemical selectivity, sensitivity, and spatiotemporal resolution and have permitted chronic and multimodal applications via advances in probe fabrication and detection methods (Huffman and Venton, 2009; Zhou et al., 2015; Al-Hasani et al., 2018; Yang et al., 2015; Ngernsutivorakul et al., 2018; Seaton et al., 2020; Feng et al., 2019b; Oh et al., 2016; Owesson-White et al., 2016; Frank et al., 2019). For example, the sensitivity and specificity of FSCV recordings have been improved using alternative waveforms and data analysis (Puthongkham and Venton, 2020; Rodeberg et al., 2016; Schmidt and McElligott,



2019). Microlithography manufacturing of smaller microdialysis probes with reduced sampling volumes (nanoliter) enables temporal sampling resolution on the scale of a few seconds when combined with segmentation of dialysates (Puthongkham and Venton, 2020). In addition, engineered aptamers combined with field effect transistors have also been used to sense NMs in solutions with high specificity and sensitivity (Nakatsuka et al., 2018). Nevertheless, despite superior sensitivity or chemical selectivity, these analytic approaches are not yet suitable to study NM release events with single cell or synapse resolution *in vivo*.

Optical approaches, on the other hand, have become more appealing to neuroscientists, as they are relatively non-invasive and promise higher spatiotemporal resolution compared to analytic chemical methods. A large number of molecular probes, such as small molecule dyes (e.g., radiolabeled metabolites, receptor agonists, or antagonists for positron emission tomography imaging) (Tuominen et al., 2014) and protein-based probes, have been developed for macro-scale imaging *in vivo*. For example, paramagnetic metalloproteins are MRI contrast agents that are amenable to protein engineering strategies for the development of ligand-sensitive MRI probes for molecular imaging. A family of MRI contrast agents based on bacterial cytochrome P450-BM3 heme domain (BM3 h) has been developed and used for quantitative, non-invasive mapping of DA release in deep brain regions with molecular specificity and high spatiotemporal resolution (a spatial resolution less than 100 μm and a temporal resolution of seconds) (Li and Jasanoff, 2020; Ghosh et al., 2018). Despite the advancement of fMRI probes and their human compatibility, spatial and temporal resolution in optimized *in vivo* preparations for fMRI still fall short of the threshold required to image signaling events at single synapses by at least two orders of magnitude.

As fluorescence microscopy systems based on one-photon (1P) or multi-photon excitation have been developed and optimized to enhance imaging depth, speed, and spatial resolution and made accessible for routine lab applications, an array of NT and NM probes, ranging from small molecules (e.g., fluorescent false NTs [Gubernator et al., 2009; Henke et al., 2018; Meszaros et al., 2018; Rodriguez et al., 2013]), small molecule-protein hybrids (e.g., EOS [Namiki et al., 2007] and Snifit [Masharina et al., 2012]), synthetic nanosensors (e.g., near infrared catecholamine nanosensor [Beyene et al., 2019; Jeong et al., 2019]), cell-based sensors (e.g., CNiFERs [Muller et al., 2014]), and protein-based approaches (e.g., i-Tango [Lee et al., 2017]), have also been developed to be compatible with fluorescence microscopy to study synaptic or volume transmissions (for review please see Liang et al., 2015) *in vitro*, *ex vivo* and *in vivo*. Recently, to further improve the imaging resolution, fluorescence protein-based sensors that report transients of NT/NMs (e.g., dLight1 and GRAB family) have been developed for direct, long-term imaging *in vivo* (for review see Andreoni et al., 2019). Fast dissemination of these optical tools has provided new opportunities to investigate NM release mechanisms and biology using microscopy and fiber-photometry. Here, we mainly focus on recent developments and applications of genetically encoded indicators for measuring NM release *in vivo*.

DESIGN OF GENETICALLY ENCODED INDICATORS OF NEURAL ACTIVITY

Protein-based sensors typically consist of an analyte-binding or sensing domain and a reporter element based on either a single fluorescent protein (FP) or two FPs. In the case of two FP-based sensors, the FPs have overlapping excitation and emission spectra, and the conformational changes in the analyte-binding or sensing domain move the two FPs into sufficient proximity for Förster Resonance Energy Transfer (FRET) to occur between them. In this case, the readout is a ratio of the intensities of the two FPs or the fluorescence lifetime of the donor FP (Lindenburg and Merckx, 2014). In the case of single FP sensors, changes in the cellular environment detected by the analyte-binding or sensing domain alter the chromophore environment of the FP, leading to an increase or decrease in fluorescence intensity (Kostyuk et al., 2019).

The main advantage of these sensors over small molecule-based fluorophores stems from their genetic encoding, which enables reporters to be constructed from proteins that are evolutionarily designed to respond to neural activity. This allows them to be optimized by computational modeling and directed evolution. Furthermore, they can be selectively expressed in cells with specific anatomical connectivity or molecular properties. Finally, these sensors can be stably expressed over long periods of time (from days to months), allowing neuroscientists to study how patterns of neural activity change with learning, development, or disease progression.

The development and refinement of genetically-encoded calcium (GECI) and voltage (GEVI) indicators advanced our capabilities in sensor design, optimization, characterization, and validation as well as our understanding of how to apply these tools in behaving animals (Carandini et al., 2015; Mollinedo-Gajate et al., 2019; Panzera and Hoppa, 2019; Yang and St-Pierre, 2016; Bando et al., 2019; Broussard et al., 2014; St-Pierre et al., 2015; Knöpfel and Song, 2019). This know-how paved the way for the development of genetically encoded indicators for other ligands, permitting several platforms to move efficiently from initial concept to functional protein sensors. Indeed, recognizing the power of the subsecond temporal and subcellular spatial resolutions enabled by single-FP-based sensors, we and others have now extended these approaches to design genetically encoded sensors for NTs and NMs. These sensors are generally categorized by two major ligand-binding scaffolds: bacterial periplasmic binding proteins (PBPs) and G-protein coupled receptors (GPCRs) (Table 1; Figures 1A and 1B).

FROM GLUTAMATE AND GABA TO NEUROMODULATORS: PBP-BASED GENETICALLY ENCODED INDICATORS

Microbial PBPs form a large protein superfamily that binds numerous classes of small molecules and peptides. Ligand binding in PBPs induces a large Venus-flytrap-like conformational change, which is highly conserved and facilitates homology modeling for sensor design and engineering based on PBPs without solved structures (Dwyer and Hellinga, 2004). This large conformational change upon ligand binding serves as the basis

Table 1. Overview of Genetically Encoded Indicators for Neurotransmitters and Neuromodulators

Sensor	Scaffold Selectivity	Specificity fold ^a	Ex/Em (nm)	$\Delta F/F_0$ max (%)	EC50 (μ M)	Detection range	On rate (ms) ^b	Off rate (ms) ^b	Applications <i>in vivo</i> , brain regions, behaviors	Ref.
iGluSnFR	Glut, Glu	1.3 (Asp)	490/510	450 ^c / 100 ^d	4.9	1 μ M–10 mM	15	92	<i>C. elegans</i> , zebrafish, mouse	Helassa et al., 2018; Marvin et al., 2013
SF-iGluSnFR-A184S	Glut, Glu	NA	490/510	310 ^c / 69 ^d	0.6	1 μ M–10 mM	85	450	Mouse, ferret	Marvin et al., 2018
iGlu _u	Glut, Glu	0.1 (Asp)	490/510	380 ^c / 170 ^e	53	10 μ M–10 mM	0.7	2.6	NA	Helassa et al., 2018
iGABASnFR	Pf622, GABA	55.5 (Gly)	485/510	250 ^c / 75 ^d	30	1 μ M–10 mM	~25 ^f	~60 ^f	Zebrafish, mouse	Marvin et al., 2019
iAChSnFR	X513-OpuBC, ACh	35 (Ch); ~1 (Nicotine)	485/510	1200 ^c / 450 ^d	2	0.1–100 μ M	~25	~60	Zebrafish, mouse	Borden et al., 2020
iNicSnFR	OpuBC, Nicotine	~1 (ACh); 4.9 (Ch)	485/535	1450 ^c / 300 ^e	10	1 μ M–10 mM	~1000	NA	NA	Shivange et al., 2019
iSeroSnFR	OpuC, 5-HT	8 (Tryptamine)	490/512	800 ^c / 1700 ^d	300	330 pm–5 mM	0.5	4	Mouse	Unger et al., 2019
dLight1.1	DRD1, DA	70 (NE); 40 (epinephrine)	490/516	230 ^e / 180 ^d	0.33	10 nM–10 μ M	10	100	Mouse	Patriarchi et al., 2018
dLight1.2	DRD1, DA	70 (NE); 40 (epinephrine)	490/516	340 ^e / 300 ^d	0.77	10 nM–10 μ M	9.5	90	Mouse	Patriarchi et al., 2018
dLight1.3b	DRD1, DA	70 (NE); 40 (epinephrine)	490/516	~900 ^e	1.6	100 nM–100 μ M	NA	NA	Mouse, rat	Patriarchi et al., 2018
dLight1.4	DRD4, DA	70 (NE); 40 (epinephrine)	490/516	~200 ^e	0.004	1 nM–1 μ M	NA	NA	Mouse, rat	Patriarchi et al., 2018
nLight1.3	B2AR, NE	50(DA)	490/516	~150 ^d or e?	0.75	0.1–100 μ M	NA	100	Mouse	Oe et al., 2020
sLight1.3	5-HT2A, 5-HT	NQ	490/516	80 ^d or e?	0.65	1 nM–10 μ M	NA	NA	Mouse	Patriarchi et al., 2018
GRAB _{DA1m}	DRD2, DA	10 (NE)	490/510	90 ^{d,e}	0.13	10 nM–1 μ M	80	3100	Mouse	Sun et al., 2018
GRAB _{DA1 h}	DRD2, DA	10 (NE)	490/510	90 ^{d,e}	0.01	1 nM–10nM	110	17150	Mouse	Sun et al., 2018
GRAB _{5-HT}	5-HT _{2C} , 5-HT	NQ	490/510	250 ^e / 280 ^d	0.022	1 nM–1 μ M	200	3130	Mouse	Wan et al., 2020
GACH2.0	M ₃ R, ACh	NQ	490/510	90 ^{d,e}	2	1–100 μ M	280 ^e	760 ^e	Mouse	Jing et al., 2018
GRAB _{NE1m}	α 2AR, NE	350 (DA)	490/510	230 ^{d,e}	0.93	0.1–100 μ M	72 ^e	680 ^e	Mouse, zebrafish	Feng et al., 2019a
SF-Venus-iGluSnFR	Glut, Glu	NA	515/528	200 ^c / 66 ^d	2.0	1 μ M–10 mM	NA	NA	Mouse	Marvin et al., 2018
R-iGluSnFR1	Glut, Glu	3.5 (Asp)	562/588	–490 ^c / –35 ^d	1	1 μ M–10 mM	NA	NA	NA	Wu et al., 2018
R-dLight1	DRD1, DA	~350 (NE)	562/588	~300 ^d or e?	0.229	0.01–100 μ M	14	150	Mouse, rat	Patriarchi et al., 2020

Ex, excitation wavelength; Em, emission wavelength; $\Delta F/F_0$, maximum change in fluorescence from basal to bound states, where available measurements *in vitro* and in cells (human embryonic kidney 293 [HEK] and/or neurons, as specified) are presented; EC50, apparent affinity from *in situ* titration in mammalian cells or dissociated neurons, unless otherwise stated; NA, data not available; NQ, other molecules/neuromodulators did not show an appreciable effect.

^athe specificity fold is expressed as the ratio between the EC50 of the target and the EC50 of other molecules causing a response in the sensor (indicated in parenthesis)

^bmeasured in acute brain slice, unless stated otherwise

^cmeasured in purified protein

^dmeasured in dissociated neurons

^emeasured in HEK293 cells

^festimated from published 1 AP trace in cultured neurons

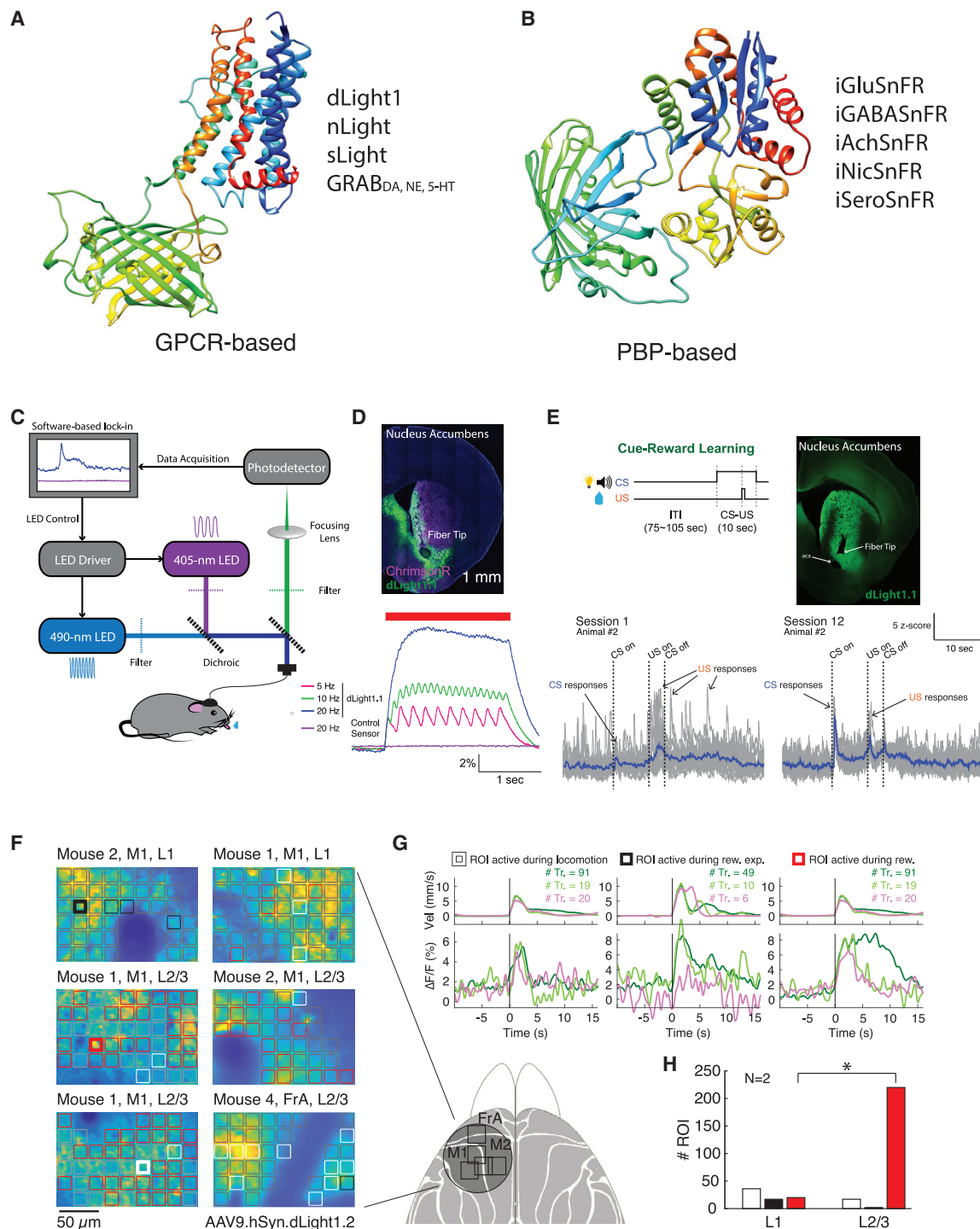


Figure 1. Development and Application of Genetically Encoded Neurotransmitter and Neuromodulator Indicators

(A and B) The design scaffolds for NT and NM indicators are based on cognate GPCR (A) or *E. coli* PBP (B). Simulated structure of dLight1.1 (A) and crystal structure of iSeroSnFR, a PBP-based serotonin sensor, without ligand binding (PDB: 6PER, B).

(C–E) Imaging DA release with dLight1.1 in behaving animals using fiber photometry.

(C) Schematic representation of fiber-photometry setup (modified from Fig 3A, [Patriarchi et al., 2019](#)).

(D) Imaging DA release in NAc triggered by optogenetics. Expression of dLight1.1 in the NAc around fiber tip location and ChromsonR expressing axons from ventral tegmental area (VTA) dopaminergic cells. Averaged fluorescence increase in response to optogenetic stimuli at 5, 10, and 20 Hz photostimulation.

(E) Dynamic changes of NAc DA signaling during appetitive Pavlovian conditioning. dLight1.1 dynamics in response to conditioned (CS) and unconditioned (US) stimuli in the first and last sessions of cue-reward learning, shown in single (gray) and averaged (blue) trials ($n = 20$ trials) from a single animal.

(legend continued on next page)

for ligand sensitivity in FRET-based sensors, such as fluorescent indicator protein for glutamate FLIPE (Okumoto et al., 2005) and SuperGluSnFR (Hires et al., 2008) or the single-FP-based sensors.

The design of single-wavelength PBP-based sensors is based on inserting circularly permuted GFP (cpGFP) or other FPs into a region of the PBP in which large ligand-induced local conformational rearrangements occur. Using this design platform, highly sensitive sensors have been developed for maltose (Marvin et al., 2011), organophosphorus (Alicea et al., 2011), glutamate (Marvin et al., 2013, 2018; Helassa et al., 2018), acetylcholine (Borden et al., 2020), glucose (Hu et al., 2018; Keller et al., 2019; Mita et al., 2019), gamma-aminobutyric acid (GABA) (Marvin et al., 2019), nicotine (Shivange et al., 2019), and, more recently, the NM serotonin (Unger et al., 2019).

iGluSnFR was the first single-FP-based sensor capable of detecting the most abundant excitatory NT glutamate *in vitro* and *in vivo* with a large response and highly specific signal (Marvin et al., 2013). iGluSnFR was developed by inserting cpGFP into a loop of the interdomain hinge region of the glutamate transporter protein GltI from *E. coli*, which shares significant homology to the glutamate-binding domain from ionotropic glutamate receptors. A critical challenge in developing iGluSnFR (or designing any single-FP-based sensors) is to determine the optimal insertion site in GltI for cpGFP. This can be achieved by analyzing changes in the dihedral-bond angle of alpha carbons (i.e., bond angle formed by four sequential amino acids) upon ligand binding. To maximize the dynamic range and kinetics of fluorescence changes in response to glutamate binding, linker regions between GltI and cpGFP were optimized via site-saturated mutagenesis (SSM). Because of the close proximity of the linkers to the chromophore, those linkers are well situated to modify chromophore-solvent access and the stability of apo and bound conformations (Akerboom et al., 2012; Nakai et al., 2001). Recent protein engineering efforts have significantly improved the kinetics and affinity of iGluSnFR to broaden the dynamics and concentration range of detectable glutamate transients, thus permitting reliable *in vivo* optical measurements in single boutons and dendritic spines (Helassa et al., 2018). Color variants of iGluSnFR were produced by replacing cpEGFP with cpAzurite, cpTurquoise2, cpVenus, and cpmApple (Marvin et al., 2018; Wu et al., 2018). These variants promise fast imaging with affordable fixed wavelength femtosecond lasers and provide new opportunities for multiplex imaging in conjunction with other probes.

The development of iGluSnFR and improved variants taught us how to perform sensor optimization, characterization, and validation for imaging NTs in behaving animals, which paved the way for the development and optimization of other PBP-based sensors. For example, the GABA sensor iGABASnFR, derived from *Pseudomonas fluorescens* Pf622, permits

recording of GABA transients in mouse brains (in hippocampal slices and visual cortex) during epileptic seizures induced with pilocarpine and in zebrafish cerebellum during motor activity (Marvin et al., 2019). The ATP sensor iATPSnFR is based on the epsilon subunit of the F_0F_1 -ATP synthase from *Bacillus subtilis* and permits detection of changing levels of ATP in the cytosol of HEK cells, neurons, and astrocytes (Lobas et al., 2019). In addition, a PBP-based sensor for acetylcholine, iAChSnFR, was developed using the choline-binding OpuBC protein from *Thermoanaerobacter spX513*, which shows large fluorescence changes, fast kinetics, and insensitivity to most cholinergic drugs and has been applied *in vivo* in mice, fish, flies, and worms (Borden et al., 2020).

With advances in ligand-redesign strategy, PBP-based sensors can now be redesigned to bind to other molecules of interest when naturally occurring PBPs are not available. Using SSM combined with rational design, a highly sensitive sensor for nicotine, iNicSnFR, was developed through optimization of the binding site and the linkers between OpuBC and cpGFP. The resulting iNicSnFR shows a 10-fold increase in fluorescence (*in vitro*) upon nicotine binding and was used to observe for the first time the dynamics of nicotine entry into the endoplasmic reticulum, a phenomenon connected to the “inside-out” pathway of upregulation of acetylcholine receptors (AChRs) that contributes to drug dependency (Shivange et al., 2019).

To design binding pockets for structurally unrelated molecules, statistical machine learning combined with computational design has been applied to guide an SSM pipeline to radically alter the binding pocket specificity. Using this strategy, we developed the first PBP-based 5-HT (serotonin) sensor (iSeroSnFR) by redesigning the binding pocket of iAChSnFR, which confers >5,000-fold improvement in 5-HT affinity while eliminating choline and ACh binding. iSeroSnFR has a maximal ~17-fold fluorescence increase upon 5-HT binding and kinetics in the millisecond range. iSeroSnFR enables imaging of 5-HT dynamics associated with electrically evoked release in brain slices and single-trial behaviorally triggered endogenous release in freely moving mice. As iSeroSnFR can be targeted intracellularly, it is ideal for use with the oscillating stimulus transporter assay (OSTA) to measure human serotonin transporter (hSERT)-mediated transport. The combination of iSeroSnFR and OSTA provides a faithful, high-spatiotemporal resolution method for longitudinal measurement of bidirectional serotonin transport and drug effects. This assay will facilitate characterization of the precise mechanisms through which SERT traffics 5-HT in its many physiological settings and could enable screening for pharmacological modulators of SERT activity (Unger et al., 2019).

Future engineering efforts of PBP-based sensors are expected to expand the set of detectable NMs, such as DA, NE, and neuropeptides (NPs), improve sensitivity and dynamic range, and extend the color palette. Though it is possible to

(F and G) Two-photon imaging of DA transients during a visuomotor association task.

(F) Example fluorescence images show dLight1.2 expression pattern for different mice and recording locations: M1 cortex, layer 1 and layer 2/3; FrA cortex, layer 2/3. The computationally defined regions of interests (ROIs), colored based on their response type, are overlaid. Dorsal view of the mouse cortex with the imaging locations (square).

(G) Single-session fluorescence transients of the highlighted ROIs highlighted in (F).

(H) Significantly more reward-related responses are seen in deeper layers. Population data showing the number of ROIs with significant dLight transients in layer 1 (L1) and layer 2/3 (L2/3) of area M1 sorted by the three response types (see G, * $p < 0.05$, Binomial test) (Figures 1C–1H modified from Patriarchi et al., 2018).

reengineer the specificity and affinity of binding pockets of PBPs, it is not an easy task. Therefore, other monoamine or NP-binding proteins should be explored as scaffolds for sensor engineering. Recently, a monoamine-binding lipocalin protein was used to engineer a fast, high-affinity 5-HT sensor (G-GESS) (Zhang et al., 2020). This elegant work opens new doors for NT- and NM-sensor engineering using other scaffolds. Finally, exploring the various genetic targeting strategies to enrich the sensors on membranes or at synapses will greatly increase the signal-to-noise ratio (SNR) and extend their applications.

GPCR-BASED GENETICALLY ENCODED INDICATORS

To enable direct and specific measurements of diverse types of NMs with the necessary spatiotemporal resolution, it is advantageous to design a sensor with molecular specificity, affinity, and kinetics similar to endogenous receptors. G-protein coupled receptors (GPCRs) are native NM targets and consist of a large superfamily of membrane proteins. Although each class has different functions, the structural features are conserved: each GPCR has seven transmembrane helices (TM1–TM7), three extracellular loops (ECL1–ECL3), an extracellular N terminus composing the ligand binding site (the most structurally variable part of the protein), three intracellular loops (ICL1–ICL3), and an intracellular C terminus that couples to effector proteins (Venkatakrishnan et al., 2013). When bound to a ligand, a cascade of conformational rearrangements occurs within the transmembrane helices, which leads to the largest motion in TM6 and transition of ICL3 from a disordered to an ordered state, a crucial step in recruiting G-proteins (Hilger et al., 2018; Sarkar et al., 2019; Weis and Kobilka, 2018; Manglik et al., 2015). These conformational changes were exploited by pharmacologists and structural biologists to drive movements of FPs and reveal mechanistic details of GPCR protein activation, kinetics, and drug response (Kauk and Hoffmann, 2018; Masureel et al., 2018; Liu et al., 2019b, 2020; Huang et al., 2020; Manglik et al., 2016; Krumm and Roth, 2020). The conformational changes of GPCRs have also been used to engineer sensors. For example, an FP acting as a FRET donor (e.g., CFP) inserted in ICL3 and a second FP acting as a FRET acceptor (e.g., YFP) linked to the C terminus can generate a FRET-based sensor. Relative motions of the loop and the C terminus upon ligand binding induce FRET between CFP and YFP. The conformational change of membrane receptors has been previously explored to engineer voltage indicators (Siegel and Isacoff, 1997).

Similarly, we leveraged such conformational changes to design an NM sensor based on protein engineering of the cognate GPCRs (Patriarchi et al., 2018). The ligand specificity, affinity, and binding kinetics that have evolved in the GPCR family provide a universal platform to design sensors for nearly any desired NM or drug. Using this design platform, we engineered dLight1, a suite of intensity-based genetically encoded indicators for DA, by replacing the ICL3 of various DA receptors with cpGFP, which maximizes the coupling of conformational changes of the receptor upon ligand binding to fluorescence changes without interfering with membrane trafficking (Patriarchi et al., 2018). The dLight1 family consists of six sensors based on

three signaling-inert DA receptors (DRD1, DRD2, and DRD4) with broadly tunable affinity, dynamic range, and fast kinetics (milliseconds) to probe DA transients across the pM– μ M range. dLight1 offers fast temporal resolution, matching that of electrochemical methods for detecting monoamines, while also providing cellular or subcellular resolution and high molecular specificity (Figure 1C). These properties of dLight1 enable robust and chronic detection of physiologically or behaviorally relevant DA transients, opening new doors to study how NMs govern rapid changes in activity and brain state (Augustine et al., 2019; Mohebi et al., 2019; de Jong et al., 2019; Robinson et al., 2019; Dong et al., 2019). Using a similar design platform, we also engineered indicators based on inert GPCRs for other NMs, including norepinephrine, serotonin, melatonin, and opioids (Patriarchi et al., 2018, 2019; Oe et al., 2020).

Using a similar approach, Sun et al. also developed the GPCR-activation-based DA sensor series (GRAB_{DA}) based on DRD2 (Sun et al., 2018). dLight1 and GRAB_{DA} use different linkers and ICL3 insertion sites, leading to different sensor properties. The GRAB family was recently enlarged by developing probes for norepinephrine (Feng et al., 2019a), serotonin (Wan et al., 2020), and acetylcholine (Jing et al., 2018) (GRAB_{NE}, GRAB_{5-HT}, and GRAB_{ACh}) based on alpha-adrenergic receptor, serotonin 2C receptor, and human muscarinic receptor 3, respectively, as sensing moieties. These sensors are also suitable for *in vivo* imaging of NMs and thus greatly expanded the toolbox of NM sensors. Compared to dLight1, in which the whole ICL3 was replaced with cpGFP, GRAB sensors contain a partial ICL3, which may not completely suppress downstream signaling as evidenced by a weak activation of the G_q-dependent calcium signaling pathway observed in GRAB_{ACh}. A side-by-side comparison of sensors' properties between dLight and GRAB family under exactly the same experimental condition across various species will provide useful information for users.

GPCR-based sensors only report the location and timing of transient NM exposure: they are signaling-inert (e.g., they do not or minimally engage either G-protein or beta-arrestin pathways) and respond with a change in fluorescence. Because the response is intrinsic to the sensor itself and does not depend on downstream coupling, it is possible to obtain useful information even with sensors expressed at levels higher than that of the endogenous GPCR or in cells that do not normally express the receptor. In cell culture, we estimated that dLight1 is overexpressed by at least 10-fold relative to endogenous GPCRs, and that this is necessary to achieve sufficient SNR with available imaging methods. As overexpressing any sensor might perturb endogenous signaling by buffering the ligand and reducing its availability at endogenous receptors, end users must carefully evaluate each sensor's potential effect on intracellular signaling, circuit activity, and behavior in the conditions and brain regions of their experiments.

PROS AND CONS OF PBP- AND GPCR-BASED NM SENSORS

Although the abundance of natural GPCRs with a diversity of ligands is advantageous for sensor design, these GPCR-based sensors cannot be used to examine the effects of

pharmacological compounds known to bind to parent receptors. In addition, as mentioned above, a sensor with similar ligand affinity as endogenous receptors may interfere with endogenous signaling pathways, which is a particular concern with long-term expression. Furthermore, GPCR-based sensors can only be expressed on membranes, preventing their use for optical measurements of neurochemicals in arbitrary cellular and extracellular compartments, as necessary to study, for example, NM/NT transport and diffusion.

These limitations of GPCR-based sensors can be potentially mitigated by PBP or other protein-scaffold-based sensors that are bio-orthogonal to neurons (i.e., do not have evolutionarily selected endogenous binding partners due to the absence in eukaryotic genomes) and have structurally unique binding pockets. In addition, PBPs are typically stable and well-tolerated when expressed in other cell types, and the availability of genomes from hyperthermophiles allows the facile discovery of incredibly stable homologs for most given PBPs. PBP-based sensors are soluble and can be expressed in cytosol or readily targeted to membranes by fusing to a transmembrane domain (e.g., PDGFR) or to other subcellular locations using various targeting strategies. In addition, they are amenable to high-throughput screening in bacteria and easily allow detailed characterization in purified protein, including biophysical and structural determination (Marvin et al., 2011, 2013, 2018). Beyond the general features discussed here, we summarize the biophysical properties and performance of both sensor classes in Table 1. With the effort to expand the toolbox of NT/NM sensors via optimization, together with systematic characterization using various imaging modality across species, sensor engineers will provide rich resources for the end users to pick the one that best fits their application.

PRACTICAL CONSIDERATIONS FOR CHOOSING THE MOST APPROPRIATE SENSOR

For end users, choosing the most appropriate sensor at the start of a project is paramount. No one sensor alone can fill the needs of every application. Sensor selection should take into consideration technical experimental conditions such as light source, fluorescence acquisition method (1P, fiber photometry, two-photon, etc.) and speed, camera, and image analysis algorithms as well as biological conditions such as expected ligand concentrations and the cell type or model organism. To maximize the SNR, the intrinsic properties of a sensor such as its expression level, affinity, and dynamic range need to be matched to the time-course, frequency, and concentration of release events in the brain region. Furthermore, when studying transmitters that act in a point-to-point manner—i.e., from a presynaptic terminal to a typically physically associated postsynaptic terminal—it may be necessary to visualize NT/NM release at each synapse individually. In other cases, in particular for transmitters that accumulate in and diffuse through the extracellular space and thus signal via volume transmission, it may be sufficient to examine the “bulk” signal generated by NT/NM release from many terminals. For these volume-transmitting NMs (such as DA in the striatum), it is thought that the joint action of many release sites mediates physiologically relevant signaling, making the need to study individual release sites less important from a

functional point of view. Nevertheless, even for these NMs, the ability to detect release at individual terminals will enable biophysical and biochemical studies of their vesicular release mechanisms. Because each system, brain region, and cell type may have different NT/NM release patterns, a sensor with high sensitivity in one setting might not be the best fit in another. A good rule of thumb is to characterize several sensors in the context of a specific application, as they each have different strengths and weaknesses. Here we discuss several practical criteria that users may wish to consider.

The apparent sensitivity of a sensor convolves together multiple biophysical parameters, most importantly apparent affinity or EC_{50} , dynamic range (F_{max}/F_{min}), on- and off-kinetics, and expression level. Specifically, a large dynamic range increases the effective concentration over which the sensor is useful. Fast on-kinetics typically increase the response to a given analyte transient, whereas fast off-kinetics decrease analyte buffering. In addition, higher expression level increases SNR but also increases buffering. An ideal sensor has fast on- and off-rates such that it is in near-instantaneous equilibrium with its ligand, rapidly couples ligand-binding to fluorescence changes, and provides high SNR signals despite being expressed at levels that bind an insignificant amount of the ligand. Furthermore, it has high molecular specificity and is insensitive to changes in concentrations of untargeted NTs, NMs, and metabolites. Having these desired properties would render the sensor quite successful in the sensitive detection of transients (even at low concentrations) without perturbing endogenous signaling.

Any exogenously expressed protein has the potential to overwhelm protein production machinery or interfere with endogenous signaling pathways (Palmer et al., 2011). Therefore, end users should first optimize the expression level of the sensor to maximize SNR under their imaging conditions. Expression level should always be as low as possible while still maintaining enough photon budget (i.e., not require more photons than can be used without inducing significant photodamage or photobleaching). To accomplish this, users may wish to explore multiple promoters such as synapsin, CAG, or CaMKII, regulatory sequences, and transduction methods (e.g., different viral serotypes and titers, stereotaxic techniques, or transgenic lines) and examine expression levels over time.

The desire to obtain a high SNR typically leads to the development of high-affinity sensors. However, high affinity is a double-edged sword, as broad expression of such sensors may buffer a large fraction of the ligand, thus dampening the amplitude and prolonging the duration of transients of free ligand available to bind endogenous receptors. In this regard, the relatively new field of NT/NM sensing can learn from the long and fruitful history of experimentation with fluorescent calcium indicators (Rose et al., 2014; Steinmetz et al., 2017; Yang et al., 2018). Because of the perturbations of calcium transients induced by calcium buffers, experiments that measure calcium transients and those that examine the cellular consequences of these transients are typically done separately—i.e., one does not typically try to measure calcium accumulation and study calcium-dependent processes at the same time (Neher and Augustine, 1992). However, we do not generally know if the buffer capacities of NT/NM sensors are functionally significant and perturb the transients of

endogenous molecules in meaningful ways. For many sensors we do not know if the kinetics of the fluorescent signal are limited by (1) the on- and off-rates of NT/NM binding to the sensor, (2) slow conformational changes in the sensor downstream of ligand binding, or (3) the kinetics of exposure to the NT/NM in the extracellular space. One hopes that (3) is true, permitting the direct estimation of NT/NM transients from fluorescence changes.

In the quest for an optimal sensor, GPCR-based and PBP-based scaffolds provide different advantages. GPCR-based sensors leverage the high evolutionary specificity of the parent GPCR for the ligand of choice, and thus naturally provide high specificity and useful affinities within the physiological range from pM to low μ M. However, they suffer from relatively low dynamic ranges and relatively slower sensor kinetics (for detailed discussion about limitations of dLight1 and variants, please see [Patriarchi et al., 2019](#); [Mizuno et al., 2019](#); [Table 1](#)). In the case of GRAB family, some high-affinity variants of GRAB_{DA} or GRAB_{5-HT} display off kinetics in the range of several seconds, which may cause ligand buffering by binding a significant fraction of the released molecules ([Wan et al., 2020](#)). Luckily, an array of naturally occurring GPCRs typically exist for each ligand, providing the possibility of creating multiple sensors with different properties, such as the dLight1 and GRAB_{DA} families, which arose from different receptors with various affinities for DA.

In contrast, most PBP-based sensors typically have affinities for their ligands that are in the μ M range, which is high compared to the extra-synaptic concentration of many NMs/NTs, and offer large dynamic ranges due to their Venus-flytrap-like closure upon ligand binding. However, they require significant engineering to optimize the affinities and specificities. Furthermore, as evolutionarily selected PBPs may not exist for many NT/NMs, challenging redesign of a binding pocket may be necessary. For both PBP- and GPCR-based sensors, it is necessary to determine a “sweet spot” at which the expression level maximizes the SNR while minimizing cellular and signaling perturbations. The best-characterized NT/NM sensors from a biophysical perspective are iGluSnFR and related glutamate reporters. The observation that expression of glutamate sensors at levels sufficient to visualize individual release events does not appear to impact the size of AMPA-receptor-mediated post-synaptic currents suggests that their buffer capacity is, in this case, not significant. This may be the case because (1) ionotropic glutamatergic transmission occurs across a narrow synaptic cleft; (2) it is mediated by the release of a relatively large number of NT molecules per vesicle (~ 3000) that likely greatly outnumbers the number of NT sensors (as it does the number of glutamate receptors, $\sim 1\text{--}100$ s); (3) the NT transient is very short lived (300–500 microseconds), possibly preventing glutamate binding to NT sensor from reaching equilibrium; and (4) there is little NT sensor in the space sampled by glutamate as it diffuses to its receptors.

On the other hand, for the study of volume signaling NMs such as DA, serotonin, and neuropeptides, the situation may be different. Sensors for these NMs are typically expressed under neuron-specific or ubiquitous promoters without targeting specific cell classes, and they typically traffic throughout the plasma membrane. Thus, the sensor is not placed at the site of action or

of high concentration of the monitored NT/NM. Since the concentration of NM reached in the extra-synaptic space is low, and the number of sensors present along the diffusion path from release site to endogenous receptor may be large, the buffer capacity of the sensor may be high. This is made more likely by the use of high-affinity sensors to detect the low concentrations of NT/NMs such that the sensors may bind a significant fraction of the released molecules, decreasing the amplitude and increasing the duration of their transients. Subcellular targeting to soma, axons, and dendrites using genetic strategies can increase the SNR of calcium and voltage sensors ([Broussard et al., 2018](#); [Piatkevich et al., 2019](#)). Similar strategies may be adapted to target NT/NMs to synapses, which will not only improve SNR by eliminating baseline brightness from regions without release but also provide an efficient solution for facile segmentation in image processing.

A recent study using simulations and electrophysiological recordings indicated that even if glutamate sensors do not alter synaptic glutamate receptor activation, the buffer capacity of the sensor does alter glia glutamate transporter currents, indicating an effect on extracellular glutamate diffusion and lifetime that likely impacts extra-synaptic receptor activation ([Armbruster et al., 2016](#)). One general way to test if such effects are caused by fast NM/NT sensors is to examine if the duration of the fluorescence transient (or ideally the physiological receptor response) depends on the level of expression of the sensor ([Tang and Yasuda, 2017](#); [Lee et al., 2017](#)). Alternatively, one could compare physiological properties of cells (such as resting potentials, membrane resistance, and capacitance) and the signaling cascades downstream of endogenous NM receptors (such as cyclic AMP [cAMP] levels, calcium transients, kinase activation, or GIRK channels) with and without sensor in the tissue. Lastly, one could examine if a behavioral or physiological effect of NT/NM release is diminished by expression of the sensor; however, this requires precise knowledge of the site of action of the NT (e.g., knowing that a particular form of DA reinforcement quantitatively depends on the action of DA specifically at the site of DA sensor expression).

CONSIDERATIONS FOR SENSOR DEVELOPERS

To engineer a GPCR- or PBP-based intensimetric sensor, the optimal insertion site of cpGFP should maximize the coupling of fluorescence changes to conformational changes induced by ligand binding. The sensitivity of a sensor depends on multiple biophysical parameters, which include dynamic range, apparent affinity, and expression level. A sensor with low affinity but high dynamic range is preferred and offers both great sensitivity and fast kinetics with a possibly reduced buffering effect. As there is no sensor that can fit all applications, it is necessary to develop a suite of sensors with various combinations of dynamic range and apparent ligand affinity. Although a prototype sensor may be relatively quick to develop, sensor optimization is an iterative process and requires a high-throughput pipeline to screen sensor properties such as brightness, dynamic range, kinetics, and apparent affinity.

SSM combined with rational or *in silico* design or guided by machine learning is effective to optimize sensor properties

such as brightness, dynamic range, kinetics, and affinity. With the availability of more advanced machine learning models and high-resolution structures of GPCRs or PBPs, it will be useful to incorporate machine learning predictions back into biophysical protein redesign, for example, using Rosetta, to improve the accuracy of prediction and prioritizing of amino acid positions and compositions for sensor optimization. However, as single mutations may only offer small improvements and combinations may give better outcomes, the mutational effects may not be additive. Therefore, performing SSM at each site separately cannot cover sufficient sequence space to radically change sensor performance. Radical improvements require simultaneous interrogation of multiple sites that are spatially distributed, which demands an efficient, high-throughput screening platform. Mammalian cell line or neuron-based screening platforms combined with robotics or single-cell microfluidics for optimizing calcium or membrane-voltage sensors provide cellular resolution conditions that are for ultimate utility *in vivo* (Wardill et al., 2013; Villette et al., 2019; Piatkevich et al., 2018). Recently, an *in situ* engineering method using CRISPR-Cas9 editing technology has been used to generate a diversified protein library in mammalian cells to screen pH-resistant FPs (Erdogan et al., 2020). Combining photolysis of caged NMs, these methods can be readily used for large-scale screening of many types of NT/NM sensors with improved properties, especially for GPCR-based sensors that are not amenable to high-throughput screening in *E. coli* as was done for calcium and PBP-based sensors. The large datasets generated from high-throughput screening will strengthen the machine learning guided approach, increasing accuracy and reliability of predictions.

To balance throughput and *in vivo* predictability, with the goal of finally demonstrating the capability of these sensors in living animals, it is important to perform systematic characterization of multiple biophysical properties (e.g., photophysical properties, molecular and pharmacological specificity, apparent affinity, dynamic range, and kinetics) in mammalian cells, in dissociated neuronal culture, and in acute brain slices. As the performance of a sensor *in vitro* may be correlated poorly with that in a more intact preparation, it is important to demonstrate its *in vivo* utility in probing behaviorally relevant NM release (see Patriarchi et al., 2019; Mizuno et al., 2019). The one- or two-photon imaging of responses to electrical stimuli in acute brain slices combined with pharmacological manipulations captures many aspects of sensor performance, such as sensitivity, specificity, and kinetics, while allowing a moderate throughput. Owing to its greater imaging depth, motion artifacts, and hemodynamics, *in vivo* imaging has more challenging SNR requirements. Therefore, it is necessary to confirm the performance of the best candidates in response to behavior or optogenetic/chemogenetic stimuli *in vivo* using multiple imaging modalities (e.g., fiber photometry, 1P, and multi-photon microscopy). To exclude the possible artifacts due to sensor's sensitivity to pH/microenvironment or hemodynamics, it is necessary to engineer and characterize a control sensor with ablated ligand binding. Alternatively, a second-best option is to use GFP fluorescence as a control, but this does not place the fluorophore in the same environment as the sensor. Finally, to better help end-users choose the most appropriate sensor, the *in vivo* performance of sensors

based on different scaffolds can be compared, but this must be done under identical conditions (e.g., promoter, expression time and level, brain regions, cell type, and stimuli).

THE CHALLENGES OF QUANTITATIVE ANALYSES OF NM TRANSIENTS

In certain cases, the analysis of fluorescence transients from NM/NT sensors can be straightforward. PBP-based glutamate sensors have sufficient dynamic range, fast kinetics, low affinity, and brightness to report glutamate release at dendrites, individual spines, or axons combined with standard (Marvin et al., 2018) or random access two-photon laser-scanning microscopy (Helassa et al., 2018) and kilohertz two-photon approaches, such as scanned line angular projection (SLAP), free-space angular-chirp-enhanced delay (FACED), or combined with direct wavefront sensing (Kazemipour et al., 2019; Wu et al., 2020; Liu et al., 2019a; Figure 2). Synaptically released glutamate generates a rapidly rising followed by an exponentially decaying fluorescence transient with a time constant of a few ms (Kazemipour et al., 2019; Helassa et al., 2018). Since, as described above, these sensors have fast kinetics and relatively low affinity, the size of the fluorescence transient approximately tracks the amount of released glutamate in a linear range. Nevertheless, the decay constant is more likely to reflect the dissociation rate of glutamate from the sensor rather than the time course of glutamate clearance. Therefore, imaging analysis typically consists of fitting exponentials to the fluorescence transients associated with each release event and extracting the amplitude and time constant of the fit. Furthermore, it is possible to increase SNR by image segmentation to limit the collection of fluorescence arising from sensors on the plasma membrane.

Unfortunately, many other PBP-based NM sensors have not been highly optimized, and GPCR-based sensors are not sufficiently fast and linear to be used in a similar manner. Such optimization will be particularly valuable for the study of NMs and neuropeptides, for which the release machinery and conditions necessary for release are poorly understood and for which it is unclear if release is regulated at the level of individual terminals. For imaging bulk signaling NMs, such as DA, single trial analysis is still possible with a variety of imaging and bulk fluorescence approaches (e.g., fiber photometry), but single vesicle release events at individual terminals are typically not visualized.

It is important to note that all fluorescent sensors generate signals that are low-pass filtered versions of the probed signals. As NT/NM release is a near-instantaneous event whereas the released molecules have some non-zero lifetime in the extracellular space, the time course of NT/NM signaling is, by definition, a low-pass filtered version of the release events. This makes it necessary to carefully consider the kinetics of targeted signaling molecules compared to that of the sensor when performing cross-correlation studies. For example, the cross-correlation of two low-pass filtered signals is artificially increased compared to the cross-correlation of the raw signals (Smith and Häusser, 2010), but the cross-correlation of a filtered signal with its own underlying raw signal continuously heads to zero as the filtering increases (Sabatini, 2019).

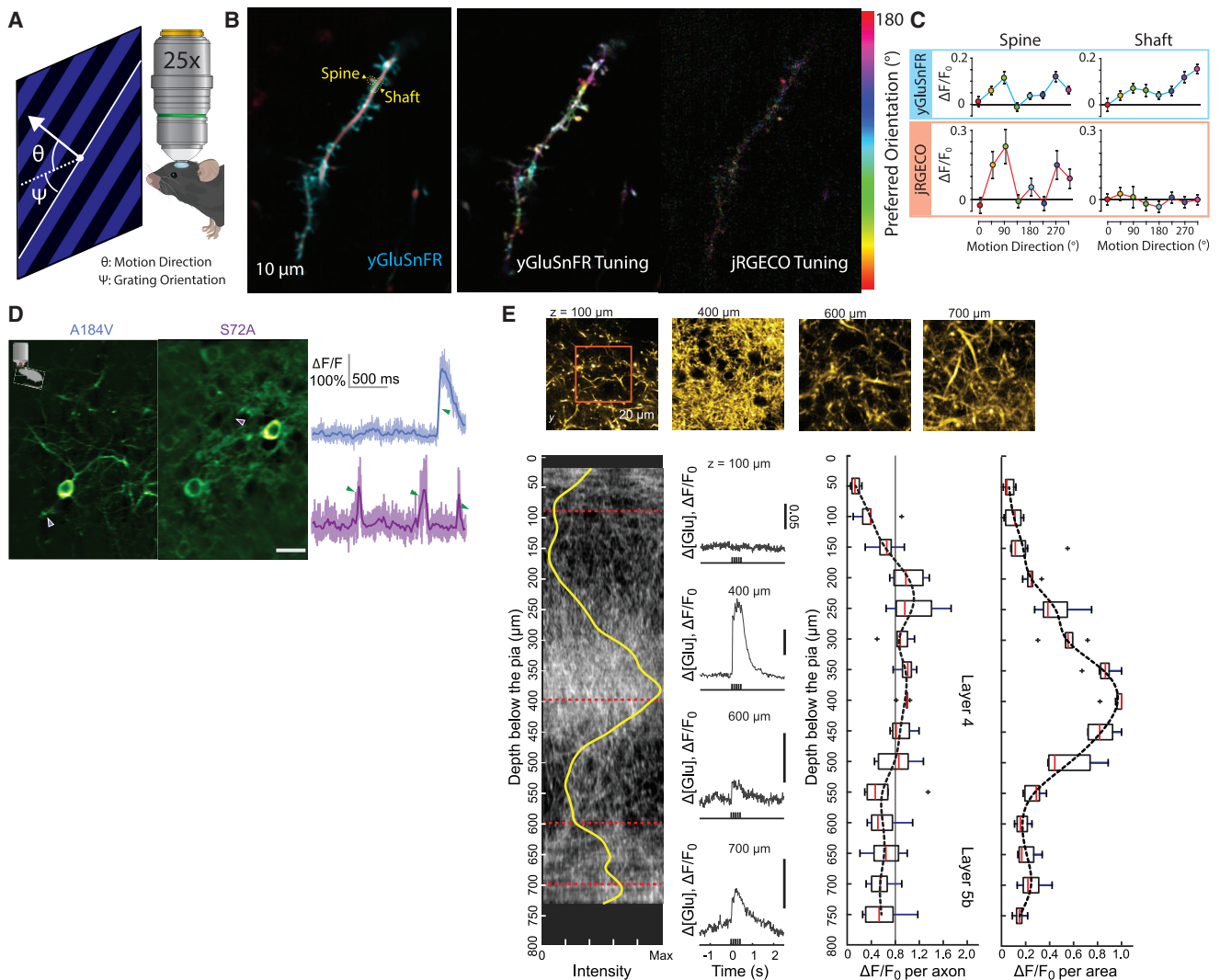


Figure 2. Kilohertz Imaging of Glutamate Release In Vivo

(A–C) Imaging glutamate release and neuronal calcium in sparsely label pyramidal neurons with SF-venus.iGluSnFR.A184S and jRGECO in response to eight directions of drifting grating motion stimuli using SLAP. Modified from Figure 4 of Kazemipour et al., (2019).

(B) Example raster image of dendrite in visual cortex co-expressing jRGECO1a (red) and SF-Venus.iGluSnFR.A184S (cyan). Pixelwise orientation tuning maps for each sensor shown on the right panel. Hue denotes preferred orientation. Saturation denotes orientation selectivity indices (OSI). Intensity denotes response amplitude. Scale bar, 10 μ m.

(C) Tuning curves for ROI outlined in (B) showed similar tuning at the spine but distinct responses in the shaft.

(D) kHz imaging of glutamate in cultured neurons and in V1 of awake mice labeled with iGluSnFR *in vivo* using FACED. Modified from Supplementary Figure 6 of Wu et al. (2020).

(E) Imaging glutamate release with SF-venus-iGluSnFR.A184S from thalamocortical axons during active tactile sensing using two-photon imaging combined with direct wavefront sensing. Modified from Figure 3 of Liu et al., 2019a. Left panel: a 175- μ m-thick projection in the x-z plane for one animal and the density (yellow) as an average over all images. Middle panel: time-dependent signal of glutamate release in various layers. Right panel: glutamate responses throughout the measurable depth of the cortical columns for the C1, C2, B2, and B3 vibrissae are shown as a population average of the peak amplitude of the signal per axon.

Finally, signals from NT/NM reporters can be difficult to compare quantitatively across conditions. Fluorescence transients are often normalized for comparison by calculating $\Delta F/F_0 = (F(t) - F_0)/F_0$ (i.e., the change in fluorescence relative a baseline value F_0). This requires defining a baseline and, by comparing the normalized value across conditions, imposes the assumption that the baseline is constant. However, this can confound comparisons of the amplitude of transients

evoked by behavior across recording sessions or animals, as the baseline can change across time, recording site, expression level, or optical fiber autofluorescence. Furthermore, for most reporters the “baseline” value in the absence of the sensed molecule is very low, making the F_0 term noisy. Dividing by such a noisy value introduces strong nonlinear perturbations as it turns normal distributions into long-tailed log-normal distributions. Other approaches to process the signal before comparison

across time or condition, such as normalizing to an inert fluorescence source in the tissue or calculating z-scores or d-prime, can also be problematic due to wavelength-dependent light absorption by tissue and blood, differential contributions, and bleaching of signal and autofluorescence from glass and tissue. The assumption in these approaches is that large transients related to behavioral events are dominant compared to the noise and emerge naturally by mean-subtracting signals normalized to their standard deviation. However, the signal baseline and its variance depend on imaging conditions and transgene expression and are differentially affected by illumination intensity. Furthermore, differential bleaching of the fluorophore and of autofluorescence (tissue and glass) make it necessary to perform these corrections on signals detrended for bleaching or in a rolling window. An alternative approach, which assumes some stationarity of responses across time, is to use dynamic range normalization—i.e., over a rolling window, define a range of signal from 0 to 1, corresponding to, for example, from the 1st percentile to the 99th percentile of the signal, and then use this normalized signal to average and compare across conditions. For all these reasons, best practices for quantification and comparison of NM/NT sensor fluorescence transients are still being formulated, and strict controls for signal generation (e.g., recordings with point mutants that abolish the NT/NM-dependent signals), acquisition (e.g., parallel recordings of NT/NM-inert fluorophores), and analysis (e.g., shuffled controls and bootstrapping) are necessary.

WHAT WE HAVE LEARNED FROM *IN VIVO* OPTICAL RECORDING USING GENETICALLY ENCODED INDICATORS

In the past decade, optical approaches have provided insights in the biology of NM release. Here we mainly focus on the recent use of genetically encoded NM sensors, which is exploding, and judging by the rapid growth of their mention in preprints, a major bolus of discovery is coming in which the advantages of optical measurements—the enhanced spatiotemporal scales on which measurements are possible—will be fully exploited. The most optimized and earliest NM/NT sensors are those for DA and glutamate, and it is worth considering what has been learned by their use. This is particularly fruitful because chemical, electrochemical, or electrophysiological methods have long existed for monitoring release of these molecules; therefore, one can examine how the use of optical sensors has facilitated discovery. What follows is a brief, and by no means comprehensive, presentation of some of the classes of discoveries propelled by optical examination of activity to NM neurons and NM release.

For DA, the ease of use of optical sensors, the ability to finely target structures within the brain, and the feasibility to chronically image across the full course of the behavioral learning permits examination of changes of dopaminergic neuron activity and DA release in multiple brain areas in a manner that was theoretically possible but experimentally challenging with older methods (e.g., see Heymann et al., 2020; Mohebi et al., 2019; Robinson et al., 2019; de Jong et al., 2019; Augustine et al., 2019 for a small subset of such studies). Therefore, we now better understand that DA release in subregions of the dorsal and

ventral striatum as well as across other brain areas differentially encodes reward expectation, action, action outcome, and sensory salience and how such signals vary across conditions (Lutas et al., 2019; Yuan et al., 2019; Menegas et al., 2017; Hamilos et al., 2020; Howe and Dombeck, 2016; Howe et al., 2019). Interestingly, similar regional specialization of dopaminergic neuron activity and signal is found in fruit flies (May et al., 2020; Handler et al., 2019; Cohn et al., 2015).

A clear demonstration of what can be gained from the use of fluorescent DA sensors is found in Lutas et al. (2019), which performed simultaneous monitoring of DA levels with dLight and optical fibers implanted in the basolateral amygdala (BLA) and nucleus accumbens (NAc) of individual mice performing a task (their Figure 4). Reward-conditioned cues increase DA levels in both structures with strong trial-to-trial correlations in signal amplitude. However, cues that predicted aversive outcomes increased DA in BLA and decreased it in NAc, with no trial-to-trial anticorrelation of the signal amplitudes. Such an experiment with simultaneous DA monitoring at two sites on the same side of the brain was extremely difficult with older technologies. The simultaneous nature of the recording permits trial-by-trial analysis of signal correlations, which allows one to infer features of the underlying neurocircuitry—the reward-predicting DA released from VTA inputs to NAc and BLA must be under common circuit control, whereas the oppositely signed aversive-outcome predicting signals are likely under independent control (as opposed to the BLA signaling reflecting suppression of the source of NAc DA).

Other studies exploit the temporal resolution and high sensitivity of DA measurements to directly examine DA “ramping” and accumulation during reward approach and action initiation, as suggested by previous electrical measurements (Howe et al., 2013; Mohebi et al., 2019; Hamilos et al., 2020). On the opposite end of the spectrum, chronic recording in individual animals reveals diurnal variations in NM levels across brain states as well as the continuous evolution of DA-dependent signaling as an animal learns a task (Dong et al., 2019; Lee et al., 2019).

For glutamate, NT sensors provide functionality that was difficult to achieve with electrophysiological measurements of synaptic currents or optical measurements of post-synaptic activity. In particular, the advantages are clear for *in vivo* use, where long-term measurements of synaptic currents are difficult for simultaneously monitoring release at multiple synapses and for probing the quantal nature of synaptic transmission at arbitrarily chosen synapses (as opposed to the one for which minimal stimulation could be achieved by placement of a stimulating electrode). Optical measurements of glutamate release at individual synapses were previously achieved with minimal stimulation or two-photon imaging of active dendritic spines (e.g., Sabatini et al., 2002; Oertner et al., 2002; Nimchinsky et al., 2004; MacAskill et al., 2012; Higley et al., 2009; Stricker et al., 1996; Bolshakov and Siegelbaum, 1995). Now the use of widely expressed fluorescent glutamate sensors with high spatiotemporal resolution imaging permits simultaneous analysis of many synapses or long-term analyses of a few synapses with relative ease. This permits both an understanding of heterogeneity of modulation within a synaptic population, linking quantal release properties to mechanisms of plasticity and disease, and direct observation

of biophysical changes to glutamate uptake and diffusion (Hellas et al., 2018; Kazemipour et al., 2019; Sakaki et al., 2020; Vevea and Chapman, 2020; Kopach et al., 2020; Barnes et al., 2020; Soares et al., 2019; Rama et al., 2019; Koch et al., 2018; Armbruster et al., 2016; Hikima et al., 2016; Borghuis et al., 2013).

OUTLOOK

We are at a new age of NM measurement across various temporal and spatial scales. A close collaboration between sensor developers and end-users is needed to identify major applications and technical barriers to motivate and guide future sensor development and optimization. Thus, for each NM there is no one sensor that can fit all applications, and robust *in vivo* monitoring of NM release can still present challenges. This is true even for monitoring DA with dLight1 or a GRAB family sensor—the most broadly utilized NM sensors for *in vivo* monitoring with two-photon microscopy or fiber photometry. For example, nearly all studies of DA have focused on dorsal and ventral striatum brain regions where dopaminergic innervation is dense and findings are well-supported with pre-existing theories about the function of DA release. However, DA is released in numerous other brain regions, such as prefrontal cortex, substantia nigra, hippocampus, basolateral amygdala, and thalamus, where dopaminergic innervation is relatively sparse. In these areas, DA is thought to be equally important in inducing cellular, circuit, and behavior plasticity, but the mechanisms and timing of its release have not yet been explored broadly or are just beginning to be explored (Lutas et al., 2019) due to challenges imposed by sensor sensitivity.

In many brain areas, multiple NMs are released in a spatiotemporally overlapping manner and often co-released with other NMs/NTs, such that sensors with greater molecular specificity, for example, a DA sensor with ablated norepinephrine binding, are essential. Furthermore, to understand the functional heterogeneity of NM release mechanisms, including traditional action-potential vesicular release but also potentially action-potential-independent or dendritic release, we need to push the imaging resolution and sensor targeting to the subcellular level. These unsolved biological questions drive optimization of the intrinsic properties of NM/NT sensors and require matching sensor properties with the SNR and spatiotemporal resolution necessary for each experiment. Therefore, iterative improvement of current and future sensors will greatly expand the scope of applications in revealing spatiotemporal dynamics of NM release across brain regions in various model organisms, including non-human primates and other typically genetically intractable species.

As the toolbox of genetically encoded optical sensors continues to grow, it is desirable to use several sensors at the same time to simultaneously dissect the functions and interactions of multiple brain circuits. This requires additional, non-GFP-based sensor variants, including some that fluoresce at shorter or longer wavelengths. Red-shifted probes have the further advantage of fluorescing at wavelengths that suffer less from scattering and absorption, allowing for deeper and more efficient imaging *in vivo*. Red and yellow versions of the genetically encoded DA sensor dLight1 have been developed, which

allows multiplexed imaging of DA release either with neuron-type-specific calcium or glutamate monitoring. A new generation of highly sensitive red-shifted NM sensors, however, requires an effort to significantly improve existing and to identify new red FPs that are as bright and reliable as GFP. Together with the effort to expand GPCR- and PBP-based sensors to recognize more NMs and peptides, these red-shifted probes will create rich new opportunities for minimally invasive, multiplexed imaging of neurochemical signaling dynamics in complex systems in the normal brain as well as in disease states, in which many different cell types and signaling events interact and contribute to pathology.

ACKNOWLEDGMENTS

This work was supported by funding to L.T. (BRAIN Initiative U01NS090604, U01NS013522, U01NS103571, DP2MH107056, and R21NS095325 from the National Institutes of Health) and to B.S. (R37 NS046579, National Institute of Health). We thank Dr. Alessio Andreoni, Nikki Tjahjono, and Karan Mahe for discussion and careful reading of the paper.

DECLARATION OF INTERESTS

L.T. is a co-founder of Seven Biosciences.

REFERENCES

- Akerboom, J., Chen, T.W., Wardill, T.J., Tian, L., Marvin, J.S., Mutlu, S., Calderón, N.C., Esposti, F., Borghuis, B.G., Sun, X.R., et al. (2012). Optimization of a GCaMP calcium indicator for neural activity imaging. *J. Neurosci.* 32, 13819–13840.
- Al-Hasani, R., Wong, J.T., Mabrouk, O.S., McCall, J.G., Schmitz, G.P., Porter-Stransky, K.A., Aragona, B.J., Kennedy, R.T., and Bruchas, M.R. (2018). *In vivo* detection of optically-evoked opioid peptide release. *eLife* 7, e36520.
- Alicea, I., Marvin, J.S., Miklos, A.E., Ellington, A.D., Looger, L.L., and Schreier, E.R. (2011). Structure of the *Escherichia coli* phosphonate binding protein PhnD and rationally optimized phosphonate biosensors. *J. Mol. Biol.* 414, 356–369.
- Andreoni, A., Davis, C.M.O., and Tian, L. (2019). Measuring brain chemistry using genetically encoded fluorescent sensors. *Current Opinion in Biomedical Engineering* 12, 59–67.
- Armbruster, M., Hanson, E., and Dulla, C.G. (2016). Glutamate Clearance Is Locally Modulated by Presynaptic Neuronal Activity in the Cerebral Cortex. *J. Neurosci.* 36, 10404–10415.
- Augustine, V., Ebisu, H., Zhao, Y., Lee, S., Ho, B., Mizuno, G.O., Tian, L., and Oka, Y. (2019). Temporally and Spatially Distinct Thirst Satiation Signals. *Neuron* 103, 242–249.e4.
- Bando, Y., Grimm, C., Cornejo, V.H., and Yuste, R. (2019). Genetic voltage indicators. *BMC Biol.* 17, 71.
- Barnes, J.R., Mukherjee, B., Rogers, B.C., Nafar, F., Gosse, M., and Parsons, M.P. (2020). The Relationship Between Glutamate Dynamics and Activity-Dependent Synaptic Plasticity. *J. Neurosci.* 40, 2793–2807.
- Beyene, A.G., Delevich, K., Del Bonis-O'Donnell, J.T., Piekarski, D.J., Lin, W.C., Thomas, A.W., Yang, S.J., Kosillo, P., Yang, D., Prounis, G.S., et al. (2019). Imaging striatal dopamine release using a nongenetically encoded near infrared fluorescent catecholamine nanosensor. *Sci Adv* 5, eaaw3108.
- Bolshakov, V.Y., and Siegelbaum, S.A. (1995). Regulation of hippocampal transmitter release during development and long-term potentiation. *Science* 269, 1730–1734.
- Borden, P.M., Zhang, P., Shivange, A.V., Marvin, J.S., Cichon, J., Dan, C., Podgorski, K., Figueiredo, A., Novak, O., Tanimoto, M., et al. (2020). A fast genetically encoded fluorescent sensor for faithful *in vivo* acetylcholine detection in mice, fish, worms and flies. *bioRxiv*. <https://doi.org/10.1101/2020.02.07.939504>.

- Borghuis, B.G., Marvin, J.S., Looger, L.L., and Demb, J.B. (2013). Two-photon imaging of nonlinear glutamate release dynamics at bipolar cell synapses in the mouse retina. *J. Neurosci.* 33, 10972–10985.
- Broussard, G.J., Liang, R., and Tian, L. (2014). Monitoring activity in neural circuits with genetically encoded indicators. *Front. Mol. Neurosci.* 7, 97.
- Broussard, G.J., Liang, Y., Fridman, M., Unger, E.K., Meng, G., Xiao, X., Ji, N., Petreanu, L., and Tian, L. (2018). In vivo measurement of afferent activity with axon-specific calcium imaging. *Nat. Neurosci.* 21, 1272–1280.
- Carandini, M., Shimaoka, D., Rossi, L.F., Sato, T.K., Benucci, A., and Knöpfel, T. (2015). Imaging the awake visual cortex with a genetically encoded voltage indicator. *J. Neurosci.* 35, 53–63.
- Cohn, R., Morante, I., and Ruta, V. (2015). Coordinated and Compartmentalized Neuromodulation Shapes Sensory Processing in *Drosophila*. *Cell* 163, 1742–1755.
- de Jong, J.W., Afjei, S.A., Pollak Dorocic, I., Peck, J.R., Liu, C., Kim, C.K., Tian, L., Deisseroth, K., and Lammel, S. (2019). A Neural Circuit Mechanism for Encoding Aversive Stimuli in the Mesolimbic Dopamine System. *Neuron* 101, 133–151.e7.
- Dong, H., Wang, J., Yang, Y.F., Shen, Y., Qu, W.M., and Huang, Z.L. (2019). Dorsal Striatum Dopamine Levels Fluctuate Across the Sleep-Wake Cycle and Respond to Salient Stimuli in Mice. *Front. Neurosci.* 13, 242.
- Dwyer, M.A., and Hellinga, H.W. (2004). Periplasmic binding proteins: a versatile superfamily for protein engineering. *Curr. Opin. Struct. Biol.* 14, 495–504.
- Erdogan, M., Fabritius, A., Basquin, J., and Griesbeck, O. (2020). Targeted In Situ Protein Diversification and Intra-organelle Validation in Mammalian Cells. *Cell Chem. Biol.* 27, 610–621.e5.
- Feng, J., Zhang, C., Lischinsky, J.E., Jing, M., Zhou, J., Wang, H., Zhang, Y., Dong, A., Wu, Z., Wu, H., et al. (2019a). A Genetically Encoded Fluorescent Sensor for Rapid and Specific In Vivo Detection of Norepinephrine. *Neuron* 102, 745–761.e8.
- Feng, T., Ji, W., Tang, Q., Wei, H., Zhang, S., Mao, J., Zhang, Y., Mao, L., and Zhang, M. (2019b). Low-Fouling Nanoporous Conductive Polymer-Coated Microelectrode for In Vivo Monitoring of Dopamine in the Rat Brain. *Anal. Chem.* 91, 10786–10791.
- Frank, J.A., Antonini, M.-J., and Anikeeva, P. (2019). Next-generation interfaces for studying neural function. *Nat. Biotechnol.* 37, 1013–1023.
- Ganesana, M., Lee, S.T., Wang, Y., and Venton, B.J. (2017). Analytical Techniques in Neuroscience: Recent Advances in Imaging, Separation, and Electrochemical Methods. *Anal. Chem.* 89, 314–341.
- Ghosh, S., Harvey, P., Simon, J.C., and Jasanoff, A. (2018). Probing the brain with molecular fMRI. *Curr. Opin. Neurobiol.* 50, 201–210.
- Gubernator, N.G., Zhang, H., Staal, R.G., Mosharov, E.V., Pereira, D.B., Yue, M., Balsanek, V., Vadola, P.A., Mukherjee, B., Edwards, R.H., et al. (2009). Fluorescent false neurotransmitters visualize dopamine release from individual presynaptic terminals. *Science* 324, 1441–1444.
- Hamilos, A.E., Spedicato, G., Hong, Y., Sun, F., Li, Y., and Assad, J.A. (2020). Dynamic dopaminergic activity controls the timing of self-timed movement. *bioRxiv*. <https://doi.org/10.1101/2020.05.13.094904>.
- Handler, A., Graham, T.G.W., Cohn, R., Morante, I., Siliciano, A.F., Zeng, J., Li, Y., and Ruta, V. (2019). Distinct Dopamine Receptor Pathways Underlie the Temporal Sensitivity of Associative Learning. *Cell* 178, 60–75.e19.
- Heien, M.L., Phillips, P.E., Stuber, G.D., Seipel, A.T., and Wightman, R.M. (2003). Overoxidation of carbon-fiber microelectrodes enhances dopamine adsorption and increases sensitivity. *Analyst (Lond.)* 128, 1413–1419.
- Helassa, N., Dürst, C.D., Coates, C., Kerruth, S., Arif, U., Schulze, C., Wiegert, J.S., Gieves, M., Oertner, T.G., and Török, K. (2018). Ultrafast glutamate sensors resolve high-frequency release at Schaffer collateral synapses. *Proc. Natl. Acad. Sci. USA* 115, 5594–5599.
- Henke, A., Kovalyova, Y., Dunn, M., Dreier, D., Gubernator, N.G., Dincheva, I., Hwu, C., Sebej, P., Ansorge, M.S., Sulzer, D., and Sames, D. (2018). Toward Serotonin Fluorescent False Neurotransmitters: Development of Fluorescent Dual Serotonin and Vesicular Monoamine Transporter Substrates for Visualizing Serotonin Neurons. *ACS Chem. Neurosci.* 9, 925–934.
- Heymann, G., Jo, Y.S., Reichard, K.L., McFarland, N., Chavkin, C., Palmiter, R.D., Soden, M.E., and Zweifel, L.S. (2020). Synergy of Distinct Dopamine Projection Populations in Behavioral Reinforcement. *Neuron* 105, 909–920.e5.
- Higley, M.J., Soler-Llavina, G.J., and Sabatini, B.L. (2009). Cholinergic modulation of multivesicular release regulates striatal synaptic potency and integration. *Nat. Neurosci.* 12, 1121–1128.
- Hikima, T., Garcia-Munoz, M., and Arbuthnott, G.W. (2016). Presynaptic D1 heteroreceptors and mGlu autoreceptors act at individual cortical release sites to modify glutamate release. *Brain Res.* 1639, 74–87.
- Hilger, D., Masureel, M., and Kobilka, B.K. (2018). Structure and dynamics of GPCR signaling complexes. *Nat. Struct. Mol. Biol.* 25, 4–12.
- Hires, S.A., Zhu, Y., and Tsien, R.Y. (2008). Optical measurement of synaptic glutamate spillover and reuptake by linker optimized glutamate-sensitive fluorescent reporters. *Proc. Natl. Acad. Sci. USA* 105, 4411–4416.
- Howe, M.W., and Dombeck, D.A. (2016). Rapid signalling in distinct dopaminergic axons during locomotion and reward. *Nature* 535, 505–510.
- Howe, M.W., Tierney, P.L., Sandberg, S.G., Phillips, P.E., and Graybiel, A.M. (2013). Prolonged dopamine signalling in striatum signals proximity and value of distant rewards. *Nature* 500, 575–579.
- Howe, M., Ridouh, I., Allegra Mascaro, A.L., Larios, A., Azcorra, M., and Dombeck, D.A. (2019). Coordination of rapid cholinergic and dopaminergic signaling in striatum during spontaneous movement. *eLife* 8, e44903.
- Hu, H., Wei, Y., Wang, D., Su, N., Chen, X., Zhao, Y., Liu, G., and Yang, Y. (2018). Glucose monitoring in living cells with single fluorescent protein-based sensors. *RSC Advances* 8, 2485–2489.
- Huang, W., Masureel, M., Qu, Q., Janetzko, J., Inoue, A., Kato, H.E., Robertson, M.J., Nguyen, K.C., Glenn, J.S., Skiniotis, G., and Kobilka, B.K. (2020). Structure of the neurotensin receptor 1 in complex with β -arrestin 1. *Nature* 579, 303–308.
- Huffman, M.L., and Venton, B.J. (2009). Carbon-fiber microelectrodes for in vivo applications. *Analyst (Lond.)* 134, 18–24.
- Jeong, S., Yang, D., Beyene, A.G., Del Bonis-O'Donnell, J.T., Gest, A.M.M., Navarro, N., Sun, X., and Landry, M.P. (2019). High-throughput evolution of near-infrared serotonin nanosensors. *Sci Adv* 5, eaay3771.
- Jing, M., Zhang, P., Wang, G., Feng, J., Mesik, L., Zeng, J., Jiang, H., Wang, S., Looby, J.C., Guagliardo, N.A., et al. (2018). A genetically encoded fluorescent acetylcholine indicator for in vitro and in vivo studies. *Nat. Biotechnol.* 36, 726–737.
- Kauk, M., and Hoffmann, C. (2018). Intramolecular and Intermolecular FRET Sensors for GPCRs - Monitoring Conformational Changes and Beyond. *Trends Pharmacol. Sci.* 39, 123–135.
- Kazemipour, A., Novak, O., Flickinger, D., Marvin, J.S., Abdelfattah, A.S., King, J., Borden, P.M., Kim, J.J., Al-Abdullatif, S.H., Deal, P.E., et al. (2019). Kilohertz frame-rate two-photon tomography. *Nat. Methods* 16, 778–786.
- Keller, J.P., Marvin, J.S., Lacin, H., Lemon, W.C., Shea, J., Kim, S., Lee, R.T., Koyama, M., Keller, P.J., and Looger, L.L. (2019). In vivo glucose imaging in multiple model organisms with an engineered single-wavelength sensor. *bioRxiv*. <https://doi.org/10.1101/571422>.
- Kennedy, R.T. (2013). Emerging trends in in vivo neurochemical monitoring by microdialysis. *Curr. Opin. Chem. Biol.* 17, 860–867.
- Knöpfel, T., and Song, C. (2019). Optical voltage imaging in neurons: moving from technology development to practical tool. *Nat. Rev. Neurosci.* 20, 719–727.
- Koch, E.T., Woodard, C.L., and Raymond, L.A. (2018). Direct assessment of presynaptic modulation of cortico-striatal glutamate release in a Huntington's disease mouse model. *J. Neurophysiol.* 120, 3077–3084.
- Kopach, O., Zheng, K., and Rusakov, D.A. (2020). Optical monitoring of glutamate release at multiple synapses in situ detects changes following LTP induction. *Mol. Brain* 13, 39.

- Kostyuk, A.I., Demidovich, A.D., Kotova, D.A., Belousov, V.V., and Bilan, D.S. (2019). Circularly Permuted Fluorescent Protein-Based Indicators: History, Principles, and Classification. *Int. J. Mol. Sci.* 20, 4200.
- Krumm, B., and Roth, B.L. (2020). A Structural Understanding of Class B GPCR Selectivity and Activation Revealed. *Structure* 28, 277–279.
- Lee, D., Creed, M., Jung, K., Stefanelli, T., Wendler, D.J., Oh, W.C., Mignocchi, N.L., Lüscher, C., and Kwon, H.B. (2017). Temporally precise labeling and control of neuromodulatory circuits in the mammalian brain. *Nat. Methods* 14, 495–503.
- Lee, S.J., Lodder, B., Chen, Y., Patriarchi, T., Tian, L., and Sabatini, B.L. (2019). Cell-type specific asynchronous modulation of PKA by dopamine during reward based learning. *bioRxiv*. <https://doi.org/10.1101/839035>.
- Li, N., and Jasanoff, A. (2020). Local and global consequences of reward-evoked striatal dopamine release. *Nature* 580, 239–244.
- Liang, R., Broussard, G.J., and Tian, L. (2015). Imaging chemical neurotransmission with genetically encoded fluorescent sensors. *ACS Chem Neurosci.* 6, 84–93, <https://doi.org/10.1021/cn500280k>.
- Lindenburg, L., and Merkx, M. (2014). Engineering genetically encoded FRET sensors. *Sensors (Basel)* 14, 11691–11713.
- Liu, R., Li, Z., Marvin, J.S., and Kleinfeld, D. (2019a). Direct wavefront sensing enables functional imaging of infragranular axons and spines. *Nat. Methods* 16, 615–618.
- Liu, X., Xu, X., Hilger, D., Aschauer, P., Tiemann, J.K.S., Du, Y., Liu, H., Hirata, K., Sun, X., Guixà-González, R., et al. (2019b). Structural Insights into the Process of GPCR-G Protein Complex Formation. *Cell* 177, 1243–1251.e12.
- Liu, X., Kaindl, J., Karczyska, M., Stöbel, A., Dengler, D., Stanek, M., Hübner, H., Clark, M.J., Mahoney, J., Matt, R.A., et al. (2020). An allosteric modulator binds to a conformational hub in the β_2 adrenergic receptor. *Nat. Chem. Biol.* 16, 749–755.
- Lobas, M.A., Tao, R., Nagai, J., Kronschräger, M.T., Borden, P.M., Marvin, J.S., Looger, L.L., and Khakh, B.S. (2019). A genetically encoded single-wave-length sensor for imaging cytosolic and cell surface ATP. *Nat. Commun.* 10, 711.
- Lutas, A., Kucukdereli, H., Alturkistani, O., Carty, C., Sugden, A.U., Fernando, K., Diaz, V., Flores-Maldonado, V., and Andermann, M.L. (2019). State-specific gating of salient cues by midbrain dopaminergic input to basal amygdala. *Nat. Neurosci.* 22, 1820–1833.
- MacAskill, A.F., Little, J.P., Cassel, J.M., and Carter, A.G. (2012). Subcellular connectivity underlies pathway-specific signaling in the nucleus accumbens. *Nat. Neurosci.* 15, 1624–1626.
- Manglik, A., Kim, T.H., Masureel, M., Altenbach, C., Yang, Z., Hilger, D., Lerch, M.T., Kobilka, T.S., Thian, F.S., Hubbell, W.L., et al. (2015). Structural Insights into the Dynamic Process of β_2 -Adrenergic Receptor Signaling. *Cell* 161, 1101–1111.
- Manglik, A., Lin, H., Aryal, D.K., McCorvy, J.D., Dengler, D., Corder, G., Levit, A., Kling, R.C., Bernat, V., Hübner, H., et al. (2016). Structure-based discovery of opioid analgesics with reduced side effects. *Nature* 537, 185–190.
- Marvin, J.S., Schreiter, E.R., Echevarría, I.M., and Looger, L.L. (2011). A genetically encoded, high-signal-to-noise maltose sensor. *Proteins* 79, 3025–3036.
- Marvin, J.S., Borghuis, B.G., Tian, L., Cichon, J., Harnett, M.T., Akerboom, J., Gordus, A., Renninger, S.L., Chen, T.-W., Bargmann, C.I., et al. (2013). An optimized fluorescent probe for visualizing glutamate neurotransmission. *Nat. Methods* 10, 162–170.
- Marvin, J.S., Scholl, B., Wilson, D.E., Podgorski, K., Kazemipour, A., Müller, J.A., Schoch, S., Quiroz, F.J.U., Rebola, N., Bao, H., et al. (2018). Stability, affinity, and chromatic variants of the glutamate sensor iGluSnFR. *Nat. Methods* 15, 936–939.
- Marvin, J.S., Shimoda, Y., Magloire, V., Leite, M., Kawashima, T., Jensen, T.P., Kolb, I., Knott, E.L., Novak, O., Podgorski, K., et al. (2019). A genetically encoded fluorescent sensor for in vivo imaging of GABA. *Nat. Methods* 16, 763–770.
- Masharina, A., Reymond, L., Maurel, D., Umezawa, K., and Johnsson, K. (2012). A fluorescent sensor for GABA and synthetic GABA(B) receptor ligands. *J. Am. Chem. Soc.* 134, 19026–19034.
- Masureel, M., Zou, Y., Picard, L.P., van der Westhuizen, E., Mahoney, J.P., Rodrigues, J.P.G.L.M., Mildorf, T.J., Dror, R.O., Shaw, D.E., Bouvier, M., et al. (2018). Structural insights into binding specificity, efficacy and bias of a β_2 AR partial agonist. *Nat. Chem. Biol.* 14, 1059–1066.
- May, C.E., Rosander, J., Gottfried, J., Dennis, E., and Dus, M. (2020). Dietary sugar inhibits satiation by decreasing the central processing of sweet taste. *eLife* 9, e54530.
- Menegas, W., Babayan, B.M., Uchida, N., and Watabe-Uchida, M. (2017). Opposite initialization to novel cues in dopamine signaling in ventral and posterior striatum in mice. *eLife* 6, e21886.
- Meszáros, J., Cheung, T., Erler, M.M., Kang, U.J., Sames, D., Kellendonk, C., and Sulzer, D. (2018). Evoked transients of pH-sensitive fluorescent false neurotransmitter reveal dopamine hot spots in the globus pallidus. *eLife* 7, e42383.
- Mita, M., Ito, M., Harada, K., Sugawara, I., Ueda, H., Tsuboi, T., and Kitaguchi, T. (2019). Green Fluorescent Protein-Based Glucose Indicators Report Glucose Dynamics in Living Cells. *Anal. Chem.* 91, 4821–4830.
- Mizuno, G.O., Unger, E.K., and Tian, L. (2019). REAL TIME MONITORING OF NEUROMODULATORS IN BEHAVING ANIMALS USING GENETICALLY ENCODED INDICATORS. *Compendium of In Vivo Monitoring in Real-Time Molecular Neuroscience (WORLD SCIENTIFIC)*, pp. 1–18.
- Mohebi, A., Pettibone, J.R., Hamid, A.A., Wong, J.T., Vinson, L.T., Patriarchi, T., Tian, L., Kennedy, R.T., and Berke, J.D. (2019). Dissociable dopamine dynamics for learning and motivation. *Nature* 570, 65–70.
- Mollinedo-Gajate, I., Song, C., and Knöpfel, T. (2019). Genetically Encoded Fluorescent Calcium and Voltage Indicators. In *Concepts and Principles of Pharmacology*, J.E. Barrett, C.P. Page, and M.C. Michel, eds. (Cham: Springer International Publishing), pp. 209–229.
- Muller, A., Joseph, V., Slesinger, P.A., and Kleinfeld, D. (2014). Cell-based reporters reveal in vivo dynamics of dopamine and norepinephrine release in murine cortex. *Nat. Methods* 11, 1245–1252.
- Nakai, J., Ohkura, M., and Imoto, K. (2001). A high signal-to-noise Ca(2+) probe composed of a single green fluorescent protein. *Nat. Biotechnol.* 19, 137–141.
- Nakatsuka, N., Yang, K.A., Abendroth, J.M., Cheung, K.M., Xu, X., Yang, H., Zhao, C., Zhu, B., Rim, Y.S., Yang, Y., et al. (2018). Aptamer-field-effect transistors overcome Debye length limitations for small-molecule sensing. *Science* 362, 319–324.
- Namiki, S., Sakamoto, H., Iinuma, S., Iino, M., and Hirose, K. (2007). Optical glutamate sensor for spatiotemporal analysis of synaptic transmission. *Eur. J. Neurosci.* 25, 2249–2259.
- Neher, E., and Augustine, G.J. (1992). Calcium gradients and buffers in bovine chromaffin cells. *J. Physiol.* 450, 273–301.
- Ngernsutorakul, T., Steyer, D.J., Valenta, A.C., and Kennedy, R.T. (2018). In Vivo Chemical Monitoring at High Spatiotemporal Resolution Using Micro-fabricated Sampling Probes and Droplet-Based Microfluidics Coupled to Mass Spectrometry. *Anal. Chem.* 90, 10943–10950.
- Nimchinsky, E.A., Yasuda, R., Oertner, T.G., and Svoboda, K. (2004). The number of glutamate receptors opened by synaptic stimulation in single hippocampal spines. *J. Neurosci.* 24, 2054–2064.
- Oe, Y., Wang, X., Patriarchi, T., Konno, A., Ozawa, K., Yahagi, K., Hirai, H., Tsuboi, T., Kitaguchi, T., Tian, L., et al. (2020). Author Correction: Distinct temporal integration of noradrenaline signaling by astrocytic second messengers during vigilance. *Nat. Commun.* 11, 3447.
- Oertner, T.G., Sabatini, B.L., Nimchinsky, E.A., and Svoboda, K. (2002). Facilitation at single synapses probed with optical quantal analysis. *Nat. Neurosci.* 5, 657–664.
- Oh, Y., Park, C., Kim, D.H., Shin, H., Kang, Y.M., DeWaele, M., Lee, J., Min, H.K., Blaha, C.D., Bennet, K.E., et al. (2016). Monitoring In Vivo Changes in

Tonic Extracellular Dopamine Level by Charge-Balancing Multiple Waveform Fast-Scan Cyclic Voltammetry. *Anal. Chem.* 88, 10962–10970.

Okumoto, S., Looger, L.L., Micheva, K.D., Reimer, R.J., Smith, S.J., and Frommer, W.B. (2005). Detection of glutamate release from neurons by genetically encoded surface-displayed FRET nanosensors. *Proc. Natl. Acad. Sci. USA* 102, 8740–8745.

Owesson-White, C., Belle, A.M., Herr, N.R., Peele, J.L., Gowrishankar, P., Carelli, R.M., and Wightman, R.M. (2016). Cue-Evoked Dopamine Release Rapidly Modulates D2 Neurons in the Nucleus Accumbens During Motivated Behavior. *J. Neurosci.* 36, 6011–6021.

Palmer, A.E., Qin, Y., Park, J.G., and McCombs, J.E. (2011). Design and application of genetically encoded biosensors. *Trends Biotechnol.* 29, 144–152.

Panzer, L.C., and Hoppa, M.B. (2019). Genetically Encoded Voltage Indicators Are Illuminating Subcellular Physiology of the Axon. *Front. Cell. Neurosci.* 13, 52.

Patriarchi, T., Cho, J.R., Merten, K., Howe, M.W., Marley, A., Xiong, W.-H., Folk, R.W., Broussard, G.J., Liang, R., Jang, M.J., et al. (2018). Ultrafast neuronal imaging of dopamine dynamics with designed genetically encoded sensors. *Science* 360, eaat4422.

Patriarchi, T., Cho, J.R., Merten, K., Marley, A., Broussard, G.J., Liang, R., Williams, J., Nimmerjahn, A., von Zastrow, M., Gradinaru, V., and Tian, L. (2019). Imaging neuromodulators with high spatiotemporal resolution using genetically encoded indicators. *Nat. Protoc.* 14, 3471–3505.

Piatkevich, K.D., Jung, E.E., Straub, C., Linghu, C., Park, D., Suk, H.J., Hochbaum, D.R., Goodwin, D., Pnevmatikakis, E., Pak, N., et al. (2018). A robotic multidimensional directed evolution approach applied to fluorescent voltage reporters. *Nat. Chem. Biol.* 14, 352–360.

Patriarchi, T., Mohebi, A., Sun, J., Marley, A., Liang, R., Dong, C., Puhger, K., Mizuno, G.O., Davis, C.M., Wiltgen, B., et al. (2020). An expanded palette of dopamine sensors for multiplex imaging in vivo. *Nat. Methods* (2020). *Nat. Methods*. <https://doi.org/10.1038/s41592-020-0936-3>.

Piatkevich, K.D., Bensussen, S., Tseng, H.A., Shroff, S.N., Lopez-Huerta, V.G., Park, D., Jung, E.E., Shemesh, O.A., Straub, C., Gritton, H.J., et al. (2019). Population imaging of neural activity in awake behaving mice. *Nature* 574, 413–417.

Pothos, E.N., Davila, V., and Sulzer, D. (1998). Presynaptic recording of quanta from midbrain dopamine neurons and modulation of the quantal size. *J. Neurosci.* 18, 4106–4118.

Putthongkham, P., and Venton, B.J. (2020). Recent advances in fast-scan cyclic voltammetry. *Analyst (Lond.)* 145, 1087–1102.

Rama, S., Jensen, T.P., and Rusakov, D.A. (2019). Glutamate Imaging Reveals Multiple Sites of Stochastic Release in the CA3 Giant Mossy Fiber Boutons. *Front. Cell. Neurosci.* 13, 243.

Robinson, J.E., Coughlin, G.M., Hori, A.M., Cho, J.R., Mackey, E.D., Turan, Z., Patriarchi, T., Tian, L., and Gradinaru, V. (2019). Optical dopamine monitoring with dLight1 reveals mesolimbic phenotypes in a mouse model of neurofibromatosis type 1. *eLife* 8, e48983.

Rodeberg, N.T., Johnson, J.A., Bucher, E.S., and Wightman, R.M. (2016). Dopamine Dynamics during Continuous Intracranial Self-Stimulation: Effect of Waveform on Fast-Scan Cyclic Voltammetry Data. *ACS Chem. Neurosci.* 7, 1508–1518.

Rodeberg, N.T., Sandberg, S.G., Johnson, J.A., Phillips, P.E., and Wightman, R.M. (2017). Hitchhiker's Guide to Voltammetry: Acute and Chronic Electrodes for in Vivo Fast-Scan Cyclic Voltammetry. *ACS Chem. Neurosci.* 8, 221–234.

Rodríguez, P.C., Pereira, D.B., Borgkvist, A., Wong, M.Y., Barnard, C., Sonders, M.S., Zhang, H., Sames, D., and Sulzer, D. (2013). Fluorescent dopamine tracer resolves individual dopaminergic synapses and their activity in the brain. *Proc. Natl. Acad. Sci. USA* 110, 870–875.

Rose, T., Goltstein, P.M., Portuguese, R., and Griesbeck, O. (2014). Putting a finishing touch on GECIs. *Front. Mol. Neurosci.* 7, 88, <https://doi.org/10.3389/fnmol.2014.00088>.

Sabatini, B.L. (2019). The impact of reporter kinetics on the interpretation of data gathered with fluorescent reporters. *bioRxiv*. <https://doi.org/10.1101/834895>.

Sabatini, B.L., Oertner, T.G., and Svoboda, K. (2002). The life cycle of Ca(2+) ions in dendritic spines. *Neuron* 33, 439–452.

Sakaki, K.D.R., Podgorski, K., Dellazizzo Toth, T.A., Coleman, P., and Haas, K. (2020). Comprehensive Imaging of Sensory-Evoked Activity of Entire Neurons Within the Awake Developing Brain Using Ultrafast AOD-Based Random-Access Two-Photon Microscopy. *Front. Neural Circuits* 14, 33.

Sarkar, K., Joedicke, L., Westwood, M., Burnley, R., Wright, M., McMillan, D., and Byrne, B. (2019). Modulation of PTH1R signaling by an ECD binding antibody results in inhibition of β -arrestin 2 coupling. *Sci. Rep.* 9, 14432.

Schmidt, K.T., and McElligott, Z.A. (2019). Dissecting the Catecholamines: How New Approaches Will Facilitate the Distinction between Noradrenergic and Dopaminergic Systems. *ACS Chem. Neurosci.* 10, 1872–1874.

Seaton, B.T., Hill, D.F., Cowen, S.L., and Heien, M.L. (2020). Mitigating the Effects of Electrode Biofouling-Induced Impedance for Improved Long-Term Electrochemical Measurements In Vivo. *Anal. Chem.* 92, 6334–6340.

Shivange, A.V., Borden, P.M., Muthusamy, A.K., Nichols, A.L., Bera, K., Bao, H., Bishara, I., Jeon, J., Mulcahy, M.J., Cohen, B., et al. (2019). Determining the pharmacokinetics of nicotinic drugs in the endoplasmic reticulum using biosensors. *The Journal of General Physiology* 151, 738–757.

Siegel, M.S., and Isacoff, E.Y. (1997). A genetically encoded optical probe of membrane voltage. *Neuron* 19, 735–741.

Smith, S.L., and Häusser, M. (2010). Parallel processing of visual space by neighboring neurons in mouse visual cortex. *Nat. Neurosci.* 13, 1144–1149.

Soares, C., Trotter, D., Longtin, A., Béique, J.C., and Naud, R. (2019). Parsing Out the Variability of Transmission at Central Synapses Using Optical Quantal Analysis. *Front. Synaptic Neurosci.* 11, 22.

St-Pierre, F., Chavarha, M., and Lin, M.Z. (2015). Designs and sensing mechanisms of genetically encoded fluorescent voltage indicators. *Curr. Opin. Chem. Biol.* 27, 31–38.

Steinmetz, N.A., Buetfering, C., Lecoq, J., Lee, C.R., Peters, A.J., Jacobs, E.A.K., Coen, P., Ollerenshaw, D.R., Valley, M.T., de Vries, S.E.J., et al. (2017). Aberrant Cortical Activity in Multiple GCaMP6-Expressing Transgenic Mouse Lines. *eneuro* 4, ENEURO.0207-17.2017.

Stricker, C., Field, A.C., and Redman, S.J. (1996). Changes in quantal parameters of EPSCs in rat CA1 neurones in vitro after the induction of long-term potentiation. *J. Physiol.* 490, 443–454.

Sun, F., Zeng, J., Jing, M., Zhou, J., Feng, J., Owen, S.F., Luo, Y., Li, F., Wang, H., Yamaguchi, T., et al. (2018). A Genetically Encoded Fluorescent Sensor Enables Rapid and Specific Detection of Dopamine in Flies, Fish, and Mice. *Cell* 174, 481–496.e19.

Tang, S., and Yasuda, R. (2017). Imaging ERK and PKA Activation in Single Dendritic Spines during Structural Plasticity. *Neuron* 93, 1315–1324.e3.

Tuominen, L., Nummenmaa, L., Keltikangas-Järvinen, L., Raitakari, O., and Hietala, J. (2014). Mapping neurotransmitter networks with PET: an example on serotonin and opioid systems. *Hum. Brain Mapp.* 35, 1875–1884.

Unger, E., Keller, J.P., Altermatt, M., Liang, R., Yao, Z., Sun, J., Matsui, A., Dong, C., Jaffe, D.A., Hartanto, S., et al. (2019). Directed Evolution of a Selective and Sensitive Serotonin Biosensor Via Machine Learning (SSRN Electronic Journal).

Ungerstedt, U., and Hallström, A. (1987). In vivo microdialysis—a new approach to the analysis of neurotransmitters in the brain. *Life Sci.* 41, 861–864.

Venkatakrishnan, A.J., Deupi, X., Lebon, G., Tate, C.G., Schertler, G.F., and Babu, M.M. (2013). Molecular signatures of G-protein-coupled receptors. *Nature* 494, 185–194.

Venton, B.J., and Cao, Q. (2020). Fundamentals of fast-scan cyclic voltammetry for dopamine detection. *Analyst (Lond.)* 145, 1158–1168.

Vevea, J.D., and Chapman, E.R. (2020). Acute disruption of the synaptic vesicle membrane protein synaptotagmin 1 using knockoff in mouse hippocampal neurons. *eLife* 9, e56469.

- Villette, V., Chavarha, M., Dimov, I.K., Bradley, J., Pradhan, L., Mathieu, B., Evans, S.W., Chamberland, S., Shi, D., Yang, R., et al. (2019). Ultrafast Two-Photon Imaging of a High-Gain Voltage Indicator in Awake Behaving Mice. *Cell* 179, 1590–1608.e23.
- Wan, J., Peng, W., Li, X., Qian, T., Song, K., Zeng, J., Deng, F., Hao, S., Feng, J., Zhang, P., et al. (2020). A genetically encoded GRAB sensor for measuring serotonin dynamics in vivo. *bioRxiv*. <https://doi.org/10.1101/2020.02.24.962282>.
- Wardill, T.J., Chen, T.W., Schreiter, E.R., Hasseman, J.P., Tsegaye, G., Fosque, B.F., Behnam, R., Shields, B.C., Ramirez, M., Kimmel, B.E., et al. (2013). A neuron-based screening platform for optimizing genetically-encoded calcium indicators. *PLoS ONE* 8, e77728.
- Weis, W.I., and Kobilka, B.K. (2018). The Molecular Basis of G Protein-Coupled Receptor Activation. *Annu. Rev. Biochem.* 87, 897–919.
- Wightman, R.M. (2006). Detection technologies. Probing cellular chemistry in biological systems with microelectrodes. *Science* 311, 1570–1574.
- Wu, J., Abdelfattah, A.S., Zhou, H., Ruangkittisakul, A., Qian, Y., Ballanyi, K., and Campbell, R.E. (2018). Genetically Encoded Glutamate Indicators with Altered Color and Topology. *ACS Chem. Biol.* 13, 1832–1837.
- Wu, J., Liang, Y., Chen, S., Hsu, C.L., Chavarha, M., Evans, S.W., Shi, D., Lin, M.Z., Tsia, K.K., and Ji, N. (2020). Kilohertz two-photon fluorescence microscopy imaging of neural activity in vivo. *Nat. Methods* 17, 287–290.
- Yang, H.H., and St-Pierre, F. (2016). Genetically Encoded Voltage Indicators: Opportunities and Challenges. *J. Neurosci.* 36, 9977–9989.
- Yang, H., Sampson, M.M., Senturk, D., and Andrews, A.M. (2015). Sex- and SERT-mediated differences in stimulated serotonin revealed by fast microdialysis. *ACS Chem. Neurosci.* 6, 1487–1501.
- Yang, Y., Liu, N., He, Y., Liu, Y., Ge, L., Zou, L., Song, S., Xiong, W., and Liu, X. (2018). Improved calcium sensor GCaMP-X overcomes the calcium channel perturbations induced by the calmodulin in GCaMP. *Nat. Commun.* 9, 1504.
- Yuan, L., Dou, Y.N., and Sun, Y.G. (2019). Topography of Reward and Aversion Encoding in the Mesolimbic Dopaminergic System. *J. Neurosci.* 39, 6472–6481.
- Zhang, S., Li, X., Drobizhev, M., and Ai, H.-W. (2020). A Fast High-Affinity Fluorescent Serotonin Biosensor Engineered from a Tick Lipocalin. *bioRxiv*. <https://doi.org/10.1101/2020.04.18.048397>.
- Zhou, Y., Wong, J.M., Mabrouk, O.S., and Kennedy, R.T. (2015). Reducing adsorption to improve recovery and in vivo detection of neuropeptides by microdialysis with LC-MS. *Anal. Chem.* 87, 9802–9809.